

β -Nickel Hydroxide Nanosheets and Their Thermal Decomposition to Nickel Oxide Nanosheets

Zhen-Hua Liang, Ying-Jie Zhu,* and Xian-Luo Hu

State Key Laboratory of High Performance Ceramics and Superfine Microstructure, Shanghai Institute of Ceramics, Chinese Academy of Sciences, Shanghai 200050, P. R. China

Received: November 18, 2003; In Final Form: January 18, 2004

Powders of single-crystalline β -nickel hydroxide (β -Ni(OH)₂) nanosheets with the hexagonal structure have been successfully synthesized by the hydrothermal method at 200 °C using nickel acetate as the nickel source and aqueous ammonia as both an alkaline and complexing reagent. The yields of β -Ni(OH)₂ nanosheet powders were higher than 92.4%. This method is simple and low-cost for large-scale production of powders of single-crystalline β -Ni(OH)₂ nanosheets. Single-crystalline nickel oxide (NiO) nanosheets have been synthesized by thermal decomposition method at 400 °C for 2 h using single-crystalline β -Ni(OH)₂ nanosheets as the precursor. The sheet shape of β -Ni(OH)₂ was sustained after thermal decomposition to NiO. The as-prepared products were characterized by X-ray powder diffraction (XRD), transmission electron microscopy (TEM), differential scanning calorimetric analysis (DSC), and thermogravimetric analysis (TG).

Introduction

In the past decade, one-dimensional (1-D) nanostructures such as nanorods, nanowires, and nanotubes have been intensively studied due to their novel properties and potential applications as components and interconnects in nanodevices.¹ However, nanosheets have not been widely studied due to the lack of knowledge on their synthesis. Recently, nickel hydroxide (Ni(OH)₂) has aroused increasing attention due to its applications in alkaline rechargeable batteries which are most widely used in many applications ranging from power tools to portable electronics and electric vehicles. The electrochemical utilization and practical capacity of Ni(OH)₂ cathodes are directly affected by their morphology and size. The development of today's electronic industry needs much higher energy density batteries. Han et al.² reported that the capacity of the positive electrode could be significantly increased when nanophase Ni(OH)₂ was added to micrometer-size spherical Ni(OH)₂. It is expected that Ni(OH)₂ nanostructures may have potential applications in high-energy-density batteries. β -Ni(OH)₂ crystallizes with a hexagonal brucite-type structure with Ni(OH)₂ layers stacked along the *c*-axis and an interlayer distance of 4.6 Å. β -Ni(OH)₂ is often selected as the discharged-state material in the electrodes due to its stability in strong alkaline electrolyte and good reversibility when charged to β -NiOOH.³

However, there have been only a few reports on the synthesis of Ni(OH)₂ nanostructures. Gedanken et al.⁴ synthesized scalpy α -Ni(OH)₂ nanostructures using the sonochemical method. Li et al.⁵ reported the synthesis of β -Ni(OH)₂ nanostructures by the NiC₂O₄ conversion method, and the as-prepared products consisted of a mixture of nanosheets and nanorods.

NiO is a semiconductor and an antiferromagnetic material. NiO has received considerable attention recently due to its attractive applications in diverse fields, such as catalysis,^{6,7} battery cathode,^{8,9} gas sensors,^{10,11} electrochromic films,^{12,13} magnetic materials,^{14,15} active optical fibers,¹⁶ and fuel cell

electrodes.^{17,18} Therefore, to explore new synthesis methods for NiO nanosheets will find its new applications or improve existing performances. To our knowledge, there has been no report on the synthesis of NiO nanosheets.

In this paper, we demonstrate that powders of β -Ni(OH)₂ single-crystalline nanosheets can be synthesized using nickel acetate and aqueous ammonia by the hydrothermal method at 200 °C. The exclusive nanosheet morphology of single-crystalline β -Ni(OH)₂ has been achieved by this method. The preparation was carried out without using any template or seed, which avoided the subsequent complicated workup procedure for removal of the template or seed. Furthermore, NiO single-crystalline nanosheets have been successfully synthesized by the thermal decomposition method at 400 °C for 2 h using β -Ni(OH)₂ single-crystalline nanosheets as the precursor. The sheet shape of single-crystalline β -Ni(OH)₂ was sustained after thermal decomposition to NiO.

Experimental Section

Nickel acetate (Ni(CH₃COO)₂·4H₂O) (Shanghai Chemical Reagents Company) and aqueous ammonia (NH₃·H₂O) (Shanghai Lingfeng Chemical Reagents Co., Ltd.) were of analytical grade and were used as purchased without further purification. Deionized water was used as the solvent in all experiments. In a typical experiment (sample 1), 0.7 g of Ni(CH₃COO)₂·4H₂O was dissolved in 30 mL of deionized water and 1 mL of 6 M NH₃·H₂O was added dropwise during magnetic stirring. The solution was sealed into Teflon-lined autoclaves and heated at 200 °C for 5 h. After hydrothermal treatment, a green suspension was obtained. The product was separated from solution by centrifugation, washed with deionized water three times, and dried at 60 °C in a vacuum. Finally, green powder was obtained. Other samples were prepared by the procedure similar to that for sample 1, but under different conditions.

X-ray powder diffraction (XRD) patterns were recorded using a Rigaku D/max 2550V X-ray diffractometer with high-intensity Cu K α radiation ($\lambda = 1.54178$ Å) and a graphite monochro-

* Corresponding author. Fax: +86-21-52413122. E-mail: y.j.zhu@mail.sic.ac.cn.

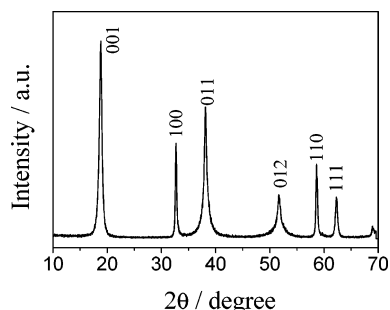


Figure 1. XRD pattern of sample 1 prepared by hydrothermally treating a solution containing 0.7 g of $\text{Ni}(\text{CH}_3\text{COO})_2 \cdot 4\text{H}_2\text{O}$, 1 mL of 6 M $\text{NH}_3 \cdot \text{H}_2\text{O}$, and 30 mL of H_2O (pH \approx 7.5) at 200 °C for 5 h. $\text{Ni}(\text{CH}_3\text{COO})_2 \cdot 4\text{H}_2\text{O}$ was dissolved in deionized water and then aqueous ammonia was added dropwise to the $\text{Ni}(\text{CH}_3\text{COO})_2$ solution during magnetic stirring before the hydrothermal treatment.

mator. TEM images were taken with JEOL JEM-2010 and JEOL JEM-200CX transmission electron microscopes. Differential scanning calorimetric analysis (DSC) and thermogravimetric analysis (TG) were carried out with a STA-409PC/4/H Luxx simultaneous TG-DTA/DSC apparatus (Germany) with a heating rate of 10 °C min^{-1} in flowing air.

Results and Discussion

Figure 1 shows the XRD pattern of a typical sample (sample 1) prepared by hydrothermally treating a solution of 0.7 g of $\text{Ni}(\text{CH}_3\text{COO})_2 \cdot 4\text{H}_2\text{O}$, 1 mL of 6 M $\text{NH}_3 \cdot \text{H}_2\text{O}$, and 30 mL of

deionized water at 200 °C for 5 h. The product was a single phase of well-crystallized β - $\text{Ni}(\text{OH})_2$ with the hexagonal structure (JCPDS 74-2075). No peaks due to α - $\text{Ni}(\text{OH})_2$ or impurities were observed by XRD. The yield of β - $\text{Ni}(\text{OH})_2$ powder was 92.4%. Other samples prepared by the hydrothermal method under different conditions have XRD patterns similar to Figure 1.

Figure 2 shows TEM micrographs of four samples prepared by the hydrothermal method. Figures 2a and 2b show TEM micrographs of the same sample (sample 1) as described in Figure 1. One can see β - $\text{Ni}(\text{OH})_2$ nanosheets as well as nanorods with diameters of 5–20 nm and lengths up to \sim 100 nm. β - $\text{Ni}(\text{OH})_2$ nanosheets have irregularly shaped morphologies with sizes in the range of 25–160 nm. Many of nanosheets are irregularly hexagonal with the angles of adjacent edges of 120° as indicated by arrows in Figure 2b. We suggest that the surface of the nanosheets is the {0001} planes of the hexagonal β - $\text{Ni}(\text{OH})_2$ phase, and the angles of 120° may be those of the {10–10} and {01–10} planes, and the edges should correspond to the {10–10} and {01–10} planes. The suggestion is supported by electron diffraction (ED) shown in Figure 2e. In addition to nanosheets, nanorods were present. The coexistence of nanosheets and nanorods was also observed by Li et al.⁵ for β - $\text{Ni}(\text{OH})_2$ synthesized by the NiC_2O_4 conversion method.

To obtain exclusive β - $\text{Ni}(\text{OH})_2$ nanosheets, we explored the influence of hydrothermal time on the product. Figure 2c shows TEM micrograph of sample 2 prepared under the same condition as sample 1 except that hydrothermal treatment time was 30 h

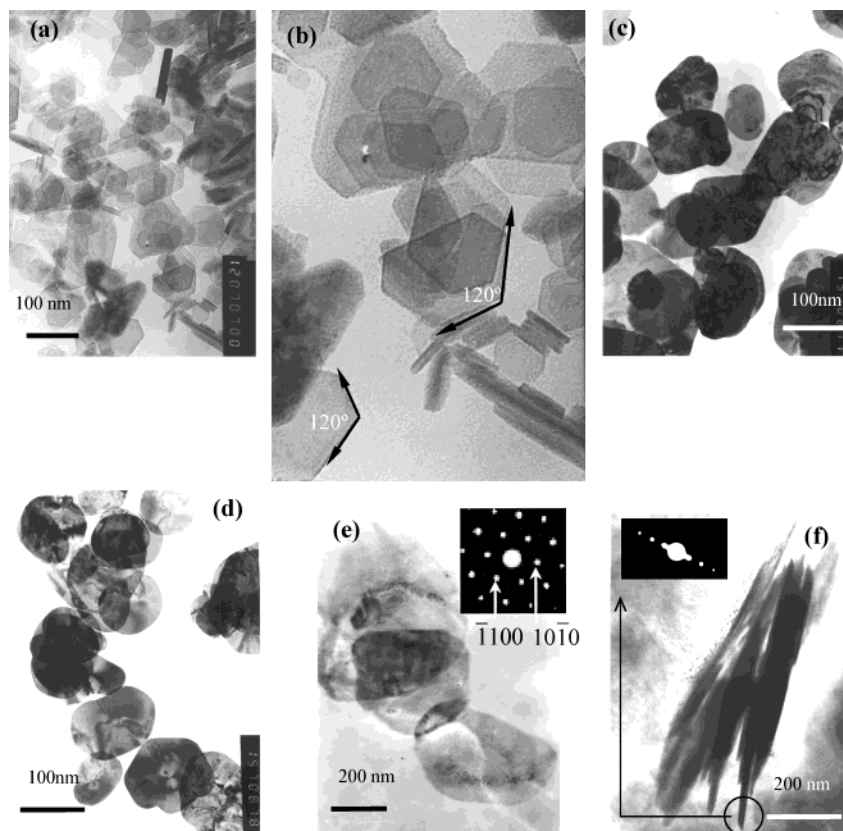


Figure 2. TEM micrographs of four samples prepared by the hydrothermal method. (a) The same sample (sample 1) as described in Figure 1; (b) the magnified TEM image for sample 1; (c) sample 2 prepared by hydrothermally treating a solution prepared as the following procedure: 0.7 g of $\text{Ni}(\text{CH}_3\text{COO})_2 \cdot 4\text{H}_2\text{O}$ was dissolved in 30 mL of H_2O , and 6 M $\text{NH}_3 \cdot \text{H}_2\text{O}$ was added dropwise to adjust the pH to 7.5. The resulting solution was hydrothermally treated at 200 °C for 30 h; (d) sample 3 prepared under the same condition as sample 2 except that pH was adjusted to 9.6; (e) sample 4 prepared by hydrothermally treating a solution prepared according to the following procedure: 0.07 g of $\text{Ni}(\text{CH}_3\text{COO})_2 \cdot 4\text{H}_2\text{O}$ and 0.016 g of poly(ethylene glycol) (PEG) was dissolved in 20 mL of H_2O , and 6 M $\text{NH}_3 \cdot \text{H}_2\text{O}$ was added dropwise to adjust the pH to 7.8. The resulting solution was hydrothermally treated at 210 °C for 33 h. The inset shows the electron diffraction pattern of a single nanosheet; (f) standing nanosheets from sample 4 on the TEM sample holder. The inset shows the electron diffraction (ED) pattern collected from the spot labeled by the circle.

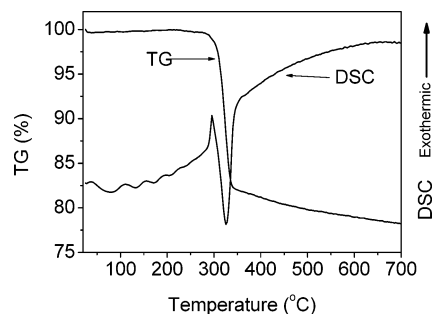


Figure 3. Differential scanning calorimetric analysis (DSC) and thermogravimetric analysis (TG) curves of β -Ni(OH)₂ nanosheets.

(5 h for sample 1). Exclusive β -Ni(OH)₂ nanosheets with sizes ranging from 50 to 160 nm were observed. No nanorods were observed. Compared with sample 1 prepared at 200 °C for 5 h, both the average size and thickness of nanosheets increased for sample 2 prepared at 200 °C for 30 h. This implies that the growth process of nanosheets occurred by increasing the hydrothermal treatment time. It is interesting to note that by increasing hydrothermal treatment time from 5 to 30 h, the shape of β -Ni(OH)₂ nanosheets had changed from irregularly hexagonal (Figures 2a and 2b) to quasi-circular (Figure 2c).

We investigated the influence of pH on the product. Samples 2 and 3 were prepared under the same condition except that pH was different. Figure 2c shows a TEM micrograph of sample 2 prepared at pH = 7.5. Exclusive nanosheets were observed. The sizes of nanosheets in sample 2 (pH = 7.5) are similar to those of sample 3 prepared at pH = 9.6. This implies that pH has limited influence on the sizes of nanosheets. We used aqueous ammonia to adjust the pH of the solution to be weak alkaline in order to provide OH⁻ ions for the formation of Ni(OH)₂. NH₃ could also act as a complexing reagent for Ni²⁺ ions to form Ni(NH₃)₆²⁺. The formation of Ni(NH₃)₆²⁺ may control the reaction rate of Ni²⁺ ions with OH⁻ ions, playing a role in the formation of β -Ni(OH)₂ nanosheets.

A TEM micrograph of sample 4 is shown in Figure 2e, which shows nanosheets with sizes of several hundred nanometers. The inset of Figure 2e shows the ED pattern of a randomly selected single nanosheet lying on the TEM sample holder, which was obtained by focusing the incident electron beam along the [0001] zone axis. ED pattern can be indexed to the hexagonal β -Ni(OH)₂, consistent with the XRD result. ED patterns taken on different individual nanosheets were essentially the same. This indicates the single-crystalline structure of β -Ni(OH)₂ nanosheets. Figure 2f shows a bundle of standing nanosheets from sample 4 on the TEM sample holder, from which we estimate that the thickness of nanosheets was in the range of ~12 to ~20 nm. The inset in Figure 2f shows the ED pattern collected from the spot labeled by the circle on a single standing nanosheet. The ED pattern was taken with an electron beam parallel with the nanosheet surface. It shows the perfect one-dimensional ED pattern, indicating a layered structure of β -Ni(OH)₂ nanosheets. The calculated spacing between Ni(OH)₂ layers stacked along the *c*-axis was about 4.7 Å, consistent with that reported (4.6 Å).¹⁹ This result supports the finding that the surface of the nanosheets is the {0001} planes of the hexagonal β -Ni(OH)₂ phase.

The thermal behavior of β -Ni(OH)₂ nanosheets was investigated with TG and DSC measurements (Figure 3). A TG curve showed that β -Ni(OH)₂ started to decompose (weight loss) at about 285 °C. The major weight loss happened rapidly between ~298 and ~342 °C. The total weight loss was measured to be

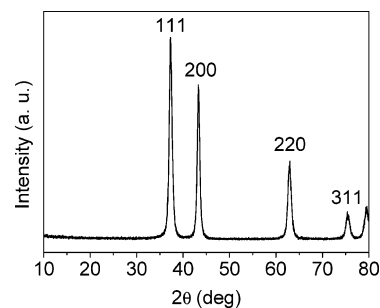


Figure 4. XRD pattern of the product (sample 5) obtained by thermal decomposition of β -Ni(OH)₂ nanosheets at 400 °C for 2 h.

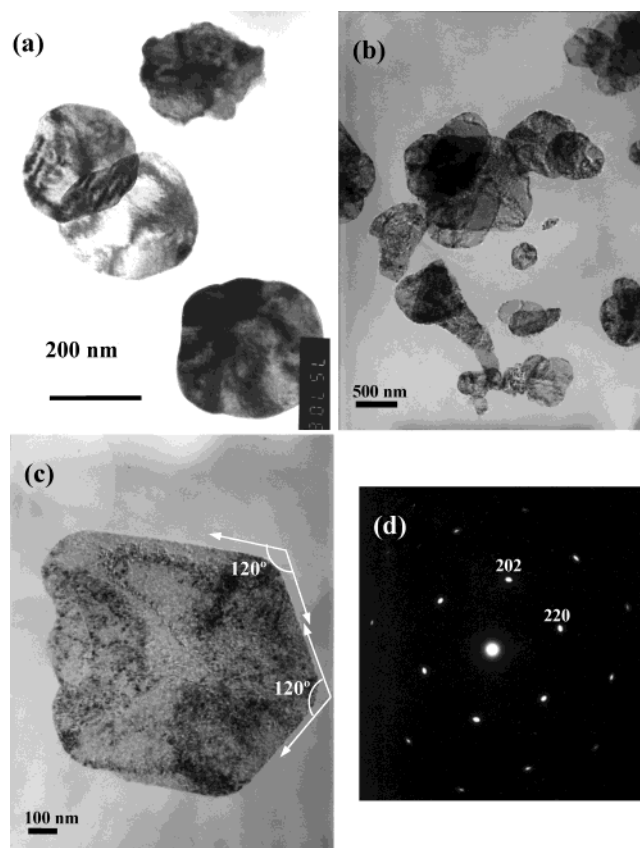
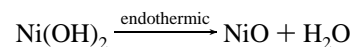


Figure 5. (a) TEM micrograph of β -Ni(OH)₂ nanosheet precursor before thermal decomposition; (b) TEM micrograph of NiO nanosheets (sample 5) obtained by thermal decomposition of β -Ni(OH)₂ nanosheets at 400 °C for 2 h; (c) a single NiO nanosheet, showing the angle of adjacent edges of 120° as indicated by arrows; (d) ED pattern of an individual NiO nanosheet.

~ 20%, in good agreement with the theoretical value (19.4%) calculated from the following reaction:



The DSC curve showed an endothermic peak with a maximum located at 326 °C. The temperature range of the endothermic peak in the DSC curve fits well with that of weight loss in the TG curve, corresponding to endothermic behavior during the decomposition of β -Ni(OH)₂ to NiO.

We explored the possibility of using β -Ni(OH)₂ nanosheets as the precursor for synthesis of NiO nanosheets. On the basis of TG and DSC results, we used 400 °C to ensure the complete decomposition of β -Ni(OH)₂. Figure 4 shows the XRD pattern of NiO powder (sample 5) prepared by thermal decomposition of single-crystalline β -Ni(OH)₂ nanosheets at 400 °C for 2 h.

All reflections in Figure 4 can be indexed to the face-centered cubic (fcc) NiO phase (space group: $Fm\bar{3}m$ [No. 225]). The lattice constant ($a = 4.173 \text{ \AA}$) is in good agreement with the reported data (JCPDS, No. 78-0643). No peaks due to β -Ni(OH)₂ were observed by XRD, indicating that β -Ni(OH)₂ was completely decomposed to NiO at 400 °C for 2 h.

The morphology of as-prepared NiO sample (sample 5) was investigated by TEM, as shown in Figure 5. Figure 5a shows the precursor single-crystalline β -Ni(OH)₂ nanosheets with sizes of ~ 200 – ~ 300 nm before thermal decomposition. Figure 5b shows NiO nanosheets with sizes up to $\sim 1 \mu\text{m}$. Figure 5c shows a single nanosheet with the angles of adjacent edges of 120° as indicated by arrows. The corresponding ED pattern is shown in Figure 5d, which was obtained by focusing the incident electron beam along the $[1\bar{1}\bar{1}]$ zone axis. It can be indexed to the fcc NiO, consistent with the XRD result. ED patterns on different individual nanosheets were essentially the same, indicating that NiO nanosheets are single-crystalline in structure.

Conclusion

Powders of single-crystalline β -Ni(OH)₂ nanosheets with the hexagonal structure have been successfully synthesized by the hydrothermal method at 200 °C. The yields of β -Ni(OH)₂ nanosheet powders were higher than 92.4%. This method is simple and low-cost for large-scale production of powders of single-crystalline β -Ni(OH)₂ nanosheets. Single-crystalline NiO nanosheets have been successfully synthesized by thermal decomposition at 400 °C using single-crystalline β -Ni(OH)₂ nanosheets as the precursor. The sheet shape of single-crystalline β -Ni(OH)₂ was sustained after thermal decomposition to single-crystalline NiO. We expect that this precursor thermal conversion method can be extended to synthesize nanosheets of other kinds of metal oxides using nanosheets of corresponding metal hydroxides as precursors.

Acknowledgment. Financial support from Chinese Academy of Sciences under the Program for Recruiting Outstanding

Overseas Chinese (Hundred Talents Program) is gratefully acknowledged. We thank the Fund for Innovation Research from Shanghai Institute of Ceramics, Chinese Academy of Sciences and the Fund from Shanghai Natural Science Foundation. We also thank Professor Meiling Ruan for assistance with TEM experiments.

References and Notes

- (1) Xia, Y. N.; Yang, P. D.; Sun, Y. G.; Wu, Y. Y.; Mayers, B.; Gates, B.; Yin, Y. D.; Kim, F.; Yan, H. Q. *Adv. Mater.* **2003**, *15*, 353.
- (2) Han, X. J.; Xie, X. M.; Xu, C. Q.; Zhou, D. R.; Ma, Y. L. *Opt. Mater.* **2003**, *23*, 465.
- (3) Dai, J. X.; Li, A. F. Y.; Xiao, T. D.; Wang, D. M.; Reisner, D. E. *J. Power Sources* **2000**, *89*, 40.
- (4) Jeevanandam, P.; Koltypin, Y.; Gedanken, A. *Nano Lett.* **2001**, *1*, 263.
- (5) Li, X. L.; Liu, J. F.; Li, Y. D. *Mater. Chem. Phys.* **2003**, *80*, 222.
- (6) Leevin, D.; Ying, J. Y. *Stud. Surf. Sci. Catal.* **1997**, *110*, 367.
- (7) Sheela, B.; Gomathi, H.; Prabhakara Rao, G. *J. Electroanal. Chem.* **1995**, *394*, 267.
- (8) Yoshio, M.; Todorov, Y.; Yamato, K.; Noguchi, H.; Itoh, J.; Okada, M.; Mouri, T. *J. Power Sources* **1998**, *74*, 46.
- (9) Yang, H. X.; Dong, Q. F.; Hu, X. H. *J. Power Sources* **1999**, *79*, 256.
- (10) Alcock, C. B.; Li, B. Z.; Fergus, J. W.; Wang, L. *Solid State Ionics* **1992**, *53*, 39.
- (11) Kumagai, H.; Matsumoto, M.; Toyoda, K.; Obara, M. *J. Mater. Sci. Lett.* **1996**, *15*, 1081.
- (12) Miller, E. L.; Rocheleau, R. E. *J. Electrochem. Soc.* **1997**, *144*, 3072.
- (13) Chigane, M.; Ishikawa, M. *J. Chem. Soc., Faraday Trans.* **1992**, *88*, 2203.
- (14) Wang, Y.; Ke, J. *High Technol. Lett.* **1997**, *3*, 92.
- (15) Felic, A. C.; Lama, F.; Piacentini, M. *J. Appl. Phys.* **1997**, *80*, 3678.
- (16) Lunkenheimer, P.; Loidl, A. *Phys. Rev. B* **1991**, *44*, 5927.
- (17) Tomczyk, P.; Mordarski, G.; Oblakowski, J. *J. Electroanal. Chem.* **1993**, *53*, 177.
- (18) Makkus, R. C.; Hemmes, K.; Wir, J. H. W. D. *J. Electrochem. Soc.* **1994**, *141*, 3429.
- (19) McEwen, R. S. *J. Phys. Chem.* **1971**, *75*, 1782.